

Nonlinear Pulse Wave Reflection at an Arterial Stenosis

T. J. Pedley

Department of Applied
Mathematics and Theoretical Physics,
Cambridge University,
Cambridge, England

A simple model is presented to analyze the effect of stenoses of different severities in a long elastic tube or artery on the pressure and flow-rate wave forms incident upon them. Wave propagation in the undisturbed tube is taken to be linear; nonlinearity arises from the quadratic dependence of stenosis pressure drop on flow rate. Before the model can be applied in practice, important physiological questions must be answered; e.g.: (a) Can the incident wave form and mean proximal pressure be regarded as given input? (b) Is the mean flow rate given, or does the peripheral resistance remain constant? Results are given on the assumption that the answer to (a) is yes. The principal conclusion is that the input impedance spectrum of a stenosed artery depends strongly on the incident wave form, as well as on the severity of the stenosis and on the distance from it at which measurements are made. There is good qualitative agreement with the results of experiments and of other models.

Introduction

There have been many investigations into the steady and unsteady fluid dynamics of arterial stenoses or laboratory models of them. Most have concentrated on either (a) the production and characteristics of turbulence in the separated flow downstream of a constriction (e.g., [1-4]), which is important both as a diagnostic sign [5, 6] and because of the deleterious effect that separation and turbulence may have on the structure of the artery wall [7, 8]; or (b) the overall pressure drops or head losses across constrictions of different severities [9-12], in assessing the extent to which peripheral perfusion is impaired or has to rely on collateral channels [13, 14].

In recent years there have also been a small number of experiments on the harmonic content of the pressure and flow-rate wave forms, not only distal to the stenosis (where both pressure and flow-rate oscillation amplitudes are reduced), but also proximal to it, where the incident wave form is modified by reflection from the stenosis and the pressure amplitude is increased [15-18]. Newman, et al. [15, 16] applied artificial stenoses to the aortae of dogs, while Farrar, et al. [17] used femoral arteries, and Rooz, et al. [18] used latex tubes. All these authors are agreed that significant changes in the wave-form shapes occur when the area ratio α_1 of the stenosis ($\alpha_1 = A_S/A_N$, where A_S = cross-sectional area at the narrowest point, A_N = normal cross-sectional area without stenosis) is less than about 0.4 (in particular the ratio of stenosed to normal modulus of input impedance, measured just proximally, increases as α_1 decreases at all measured frequencies), although there is no significant change in *mean* pressure and flow rate unless $\alpha_1 \lesssim 0.1$. Thus, observation of wave-form distortion may be a better tool for the

early diagnosis of stenoses than measurements of mean pressure and flow rate.

More quantitative aspects of these authors' data do not show the same measure of agreement, however, as the following example shows. For a stenosis in the thoracic aorta (of a dog) Newman, et al. [15] found that, with $\alpha_1 = 0.1$, the stenosed-to-normal pressure (p) and flow rate (Q) amplitude ratios, p'_S/p'_N and Q'_S/Q'_N say, were virtually independent of frequency for the first six Fourier components of the wave form, both just proximal and just distal to the stenosis. The same is therefore true of the effective (input) impedance modulus ratio, $|Z_S/Z_N|$. In the abdominal aorta, at a distance of 20 mm proximal to the stenosis ($\alpha_1 = 0.05$), Newman, et al. [16] found a small rise with frequency of Q'_S/Q'_N , and hence a fall of $|Z_S/Z_N|$. However, in the femoral artery, at a distance of 6 mm proximal to the stenosis, Farrar, et al. [17] found a significant and nonmonotonic variation of these ratios with frequency for $\alpha_1 \lesssim 0.3$: there was a marked peak of $|Z_S/Z_N|$ at the fourth harmonic. At a much greater proximal distance of 140 mm, Newman, et al. [16] found a marked *minimum* in this ratio at the third harmonic, but they showed how this was entirely consistent with the retrograde propagation of a damped reflected wave. Rooz, et al. [18] also emphasized the importance of knowing the distance from the stenosis at which measurements are made. However, as Farrar, et al. made clear, there must have been a significant difference in conditions in their canine femoral arteries and Newman, et al.'s canine aortas; the results of this paper indicate that one important difference may be the difference in harmonic content of the incident wave form, i.e., in its shape.

Such differences cannot be investigated without a theoretical model of how a stenosis affects a pressure wave incident upon it, and the simpler the model is (without becoming unrealistic), the easier it is to assess the influence of

Contributed by the Bioengineering Division for publication in the JOURNAL OF BIOMECHANICAL ENGINEERING. Manuscript received by the Bioengineering Division, November 10, 1982; revised manuscript received July 5, 1983.

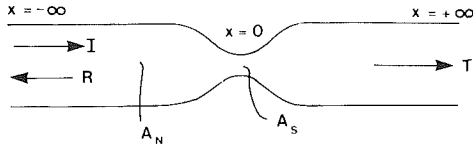


Fig. 1 Sketch of stenosis, showing direction of propagation of incident (*I*), reflected (*R*) and transmitted (*T*) waves. A_N , A_S are normal and stenosed cross-sectional areas.

various parameters on the results. The simplest possible model would be an entirely linear one, based on the theory of Womersley [19], but that would be inadequate because the pressure drop across a stenosis is known to depend nonlinearly on the flow rate. (The model of Newman, et al. [20] was effectively linear, because they took the stenosis to have a constant resistance as the flow rate varied during a cycle.) The model to be presented in this paper takes that nonlinearity into account, but still treats the wave propagation in the vessel distal and proximal to the stenosis as linear, as is approximately justified in the normal arterial system [21, 22]. The model is extremely simple, since, given the incident pressure wave form and the value of various parameters, the reflected and transmitted wave forms of pressure and flow rate can be obtained merely from the solution of a quadratic equation. On the way to the quadratic equation, however, the answers to a number of important physiological questions are required; it may be the extreme simplicity of the model which helps to throw these questions into relief.

The physical basis of the model is essentially the same as for those of Kim and Corcoran [23] and of Rooz, et al. [18], both of which agreed well with laboratory experiments on latex tubes. However, the former incorporated nonlinear wave propagation into the model, and a lengthy numerical solution was required. The latter, too, although linearizing the wave propagation, chose to solve the equations by a purely numerical, finite element method, and perhaps for that reason did not pinpoint so sharply the physiological questions that are raised. Nor did they make explicit what is perhaps the most important qualitative conclusion that can be drawn as a consequence of the system nonlinearity: that the effect of a stenosis on the pressure pulse depends not only on the degree of stenosis but also on the shape of the incident wave form itself. A given stenosis in a given tube does not lead to a unique relation between impedance and frequency, at physiological values of the parameters of the model.

The Model

We suppose that the stenosis (of narrowest area $A_S = \alpha_1 A_N$) is located in the neighborhood of $x = 0$ in a long, otherwise uniform elastic tube of undisturbed cross-sectional area A_N (Fig. 1). All waves reflected towards the stenosis from the periphery are neglected, which is equivalent to the assumption that the impedance at all distal arterial junctions is well matched. Let the speed of the wave propagation in the unstenosed tube be c and let its characteristic admittance (the inverse of characteristic impedance: see [24]) be $Y (= A_N/\rho c$, where $\rho =$ fluid density). We take these quantities to be real valued, although if viscous or visco-elastic wave attenuation is important, they will be complex and may be frequency dependent. However, we shall consider waves whose wavelength is much larger than the diameter of the tube and the length of the stenosis, and significantly larger than the distance from the stenosis at which pressures and flow rates are supposed to be measured (a low wave speed of 5 m s^{-1} and a high frequency of 15 Hz still leads to a wavelength of 33 cm). Since the attenuation per wavelength of physiological pressure waves is not large (about 50 percent: see [21]), it can

therefore be neglected in the present model. The only energy dissipation will occur at the stenosis itself.

The nonlinear analysis of the reflection of a pressure wave at the stenosis will follow the same approach as Lighthill's version of the linear theory [24]. We suppose that the pressure (p) and flow rate (Q) wave forms associated with the incident wave, arriving at the stenosis from $x = -\infty$, are given by

$$I: p = p_o[\gamma + p_I(t-x/c)], \quad Q = Q_o + Y p_o p_I(t-x/c) \quad (1)$$

Here p_I (a function of $t - x/c$ for a wave propagating to the right) is the nondimensional representation of the fluctuating part of the pressure wave form, with zero mean, and the scale factor p_o is chosen for convenience so that the peak-to-trough amplitude of p_I is 2 (like the pure cosine wave $\cos \omega t$); $p_o \gamma$ is the mean pressure proximal to the stenosis, and Q_o is the mean flow rate. In man or dog, for example, p_o would be about 2.67 kPa (20mm Hg) and γ would be about 5.0 (mean pressure ≈ 100 mm Hg). We similarly represent the reflected and transmitted waves:

$$R: p = p_o p_R(t+x/c), \quad Q = -Y p_o p_R(t+x/c) \quad (2)$$

$$T: p = p_o[\gamma' + p_T(t-x/c)], \quad Q = Q_o + Y p_o p_T(t-x/c) \quad (3)$$

where the mean distal pressure, $p_o \gamma'$, will not be the same as the proximal because of energy loss at the stenosis, but the mean flow rate must by conservation of mass still be Q_o . The fact that p_I , p_R and p_T are the fluctuating parts of the pressures, with zero mean, may be represented by the equations

$$\bar{p}_I = \bar{p}_R = \bar{p}_T = 0 \quad (4)$$

If we suppose $p_I(t)$ to be given, then $p_R(t)$ and $p_T(t)$ are to be determined by application of two equations, representing conservation of mass and the pressure-flow relation across the stenosis, respectively. We recall that the stenosis length is to be much less than a wavelength, so that (a) volume changes in the stenosed region are negligible, (b) the inertia of the fluid in the stenosis is negligible (see the forthcoming), and (c) the stenosis can be taken to be at the point $x = 0$ as far as the waves are concerned (see [24] for further justification of these approximations).

Conservation of mass states that the total flow rate on the two sides of the stenosis is the same at all times, and hence

$$p_I(t) - p_R(t) = p_T(t) \quad (5)$$

The *pressure drop* Δp across a stenosis when the flow rate through it is $Q(t)$ has been given by Young and Tsai [11] to be

$$\Delta p = \rho u^2 \left\{ K_I \cdot \frac{1}{2} \left(\frac{1}{\alpha_1} - 1 \right)^2 + \frac{K_v}{\text{Re}} + K_u \cdot \frac{L du/dt}{u^2} \right\} \quad (6)$$

where $\rho =$ fluid density, $u = Q/A_N$, $\text{Re} =$ Reynolds number based on the undistorted vessel diameter d and the velocity u , L is the effective stenosis length, and K_I , K_v , K_u are constants, representing head loss due to the separated turbulent jet at the constriction, direct viscous wall stresses, and unsteady inertia, respectively. If the stenosis consisted of a plug with a straight circular tube drilled through it, containing quasi-steady Poiseuille flow, and if the ideal Borda-Carnot conditions were applicable to the separated jet, these three constants would take the values $K_I = 1$, $K_u = 1$, $K_v = 32L/\alpha_1^2 d$. In fact they depend on stenosis geometry, and Rooz, et al. [18] quote values of $K_I = 1.52$ and $K_u = 1.2$, with an empirical modification to the length L in K_v . Equation (6) has been approximately verified for values of α_1 down to about 0.1 [11, 12]. In our case of a short stenosis ($L < 5 \text{ mm}$ in Newman, et al.'s experiments [16]) the unsteady term is negligibly small, as can be seen by taking realistic values of $L = 5 \text{ mm}$, $u = 0.1 \text{ ms}^{-1}$ (a low value), $\alpha_1 = 0.1$, $du/dt = 2\pi f u$ (the scale for a cosine wave of frequency f) and $f = 10 \text{ Hz}$ (the 5th harmonic of a dog): then the ratio of the

third term in equation (6) to the first is approximately 0.08. The viscous term will also be small if the Reynolds number is large and if α_1 is not too small. Now Re in canine aorta and femoral artery is large throughout most of systole (in the aorta, peak Re \approx 4500, mean Re \approx 800 [22]); but since we wish to consider severe stenoses with $\alpha_1 = 0.1$ and 0.05, we should retain that term in principle, although the nonlinear term will dominate. With (1), (2), (3) substituted into (6), the pressure drop equation now becomes

$$p_o[\gamma + p_I(t) + p_R(t) - \gamma' - p_T(t)] = k_2 Q |Q| + k_1 Q \quad (7)$$

where

$$Q(t) = Q_o + Y p_o p_T(t),$$

and

$$k_2 = \frac{K_I}{2} \frac{\rho}{A_N^2} \left(\frac{1}{\alpha_1} - 1 \right)^2, \quad k_1 = \frac{8\pi\mu L}{A_S^2} \quad (8)$$

with fluid viscosity $= \mu$. Note that Q^2 has been replaced by $Q|Q|$ in the jet term, to allow for the possibility of reversed flow.

In the case $Q > 0$, a combination of (5) and (7) leads to the following quadratic equation:

$$k_2 p_T^2 + 2p_T(k_2 Q_o + k_1/2 + 1/Y) + Y p_o + [k_2 Q_o^2 + k_1 Q_o - p_o(2p_I + \gamma - \gamma')]/Y^2 p_o^2 = 0, \quad (9)$$

with the sign of the k_2 terms changed whenever $Q < 0$. Thus, given the physical constants of the system (Y, p_o, k_1, k_2), given the proximal mean pressure $p_o \gamma$ and incident wave form $p_I(t)$, and given the other two constants γ' and Q_o , the transmitted wave form $p_T(t)$ (and, from (5), the reflected wave form $p_R(t)$) can be calculated as a function of time and the problem is solved. But, apart from the physical constants, it is not clear that all these quantities are given in practice.

(i) Are the incident pressure wave form $p_I(t)$ and proximal mean pressure $p_o \gamma$ given? If the stenosis is in a peripheral branch artery, so that the overall input impedance of the parent artery is virtually unchanged, then the pressure at the entrance to the branch will also be unchanged by the presence of the stenosis, so the answer is yes for the mean pressure. The incident wave form may however be modified if the wave reflected at the stenosis is significantly re-reflected at the entrance to the branch. This could be important in the femoral artery [17]. The answer is also difficult in the case of a stenosis in the aorta [15, 16] because most of the blood flow passes through it. Newman, et al. [15, 16] argued that there were no significant reflections arriving at the stenosis from either the periphery (because their animals were vasodilated) or the heart, so that the incident wave arriving from the heart was presumably unchanged; they did not discuss the mean pressure. On the other hand, Elzinga and Westerhof [25] demonstrated that the source impedance of the heart is not independent of load; and indeed the heart behaves more like a flow source than a pressure source for the lower frequency harmonics of the wave form. In modeling Newman, et al.'s experiments, then, one should presumably match the proximal end of the tube under study to a model pump, such as that of Westerhof, et al. [26], whose source impedance is the same as that of the heart. In laboratory experiments one can choose arbitrary pump characteristics: Newman, et al. [20] took the flow rate amplitude to be given, while Rooz, et al. [18] took the incident pressure wave form to be given. For the results presented here, we have followed the latter authors and taken the heart to be a pressure source, so that both $p_I(t)$ and $p_o \gamma$ are given.

(ii) How do we determine the mean flow-rate, Q_o , and mean distal pressure, $p_o \gamma'$? Whether or not the heart is a flow source, autoregulation will tend eventually to adjust the peripheral resistance so that Q_o is the same with stenosis as

without, so its value would be equal to Q_N , its normal value. On the other hand, the peripheral resistance would tend to be unchanged either immediately after the application of an artificial stenosis, or on a longer time scale if the subject was already completely vasodilated. In that case the ratio of pressure to flow rate would be unchanged, and we would have

$$Q_o = \gamma' Q_N / \gamma. \quad (10)$$

We follow Rooz, et al. [18] and consider both these choices in the forthcoming. A more complicated possibility is to suppose that the system is terminated not by a pure resistance, but by some compliance and inertance too, in order to model the distal bed more accurately [20]. However this makes the input admittance of the distal region (the Y in the second of equations (3)) frequency dependent, and equation (9) cannot be applied so simply (waves reflected from the periphery can no longer be neglected).

Equation (10) (or $Q_o = Q_N$) is one relation for the two unknowns Q_o and γ' . The other comes simply from the requirement (4) that $\bar{p}_T = 0$. The model is now complete. The results will be discussed mainly in terms of the modulus and phase of the complex effective input impedance Z_S at a distance l upstream of the stenosis ($x = -l$). If we Fourier analyze $p_I(t)$ as follows:

$$p_I(t) = \sum_{n=1}^N p_{In} \cos(n\omega t - \phi_{In}), \quad (11)$$

where ω is the fundamental angular frequency ($2\pi \times$ heart rate), with similar forms for p_R and p_T , then Z_S for the n th mode is given by

$$\frac{Z_{Sn}}{Z_{Nn}} = Y Z_{Sn} = \frac{p_{In} e^{-i\phi_{In}} + p_{Rn} e^{-i(2n\lambda + \phi_{Rn})}}{p_{In} e^{-i\phi_{In}} - p_{Rn} e^{-i(2n\lambda + \phi_{Rn})}} \quad (12)$$

where

$$\lambda = \omega l / c \quad (13)$$

In order to assess the effect of the nonlinearity, the results will be compared with those of the corresponding linear theory in which $k_2 = 0$; in that case, (9) and (5) give

$$p_T = \frac{2p_I}{2 + k_1 Y}, \quad p_R = \frac{k_1 Y p_I}{2 + k_1 Y} \quad (14)$$

with the consequence that

$$Y Z_{Sn} = \frac{2 + k_1 Y + k_1 Y e^{-i*2n\lambda}}{2 + k_1 Y - k_1 Y e^{-i*2n\lambda}} \quad (15)$$

These linear formulas can also be derived from Womersley's theory [19] for a short, straight stenosis in which viscosity is much more important than inertia (i.e., his well-known parameter α is small).

Results and Discussion

We take the physical constants of the system to have the following values, representative of the canine aorta [22], for comparison with the results of Newman, et al. [15, 16]:

$$\rho = 1.0 \times 10^3 \text{ kg m}^{-3}, \quad c = 5.0 \text{ m s}^{-1}, \quad A_N = 1.78 \times 10^{-4} \text{ m}^2$$

(hence $Y = 1/Z_N = 3.54 \times 10^{-8} \text{ m}^4 \text{ s kg}^{-1}$), $p_o = 2.67 \text{ kPa}$, $Q_N = 3.53 \times 10^{-5} \text{ m}^3 \text{ s}^{-1}$, $\omega = 4\pi \text{ s}^{-1}$ (heart rate = 2 Hz), $\gamma = 5$, $K_u = 0$. For nonlinear calculations we shall take $K_I = 1.52$ in k_2 , and $k_1 = 0$ (equation (8)), while for the corresponding linear calculations we take $k_2 = 0$ and choose k_1 so that the steady pressure drop across the stenosis is the same as in the nonlinear case at a flow rate of Q_N , i.e., $k_1 = Q_N$ times the nonlinear value of k_2 . The quantities to be varied are the area ratio α_1 , from 0.5 down to 0.02, and the proximal distance from the stenosis, l , at which pressures and flow rates are recorded: 0, 20, 70, 140 mm, as in Newman, et

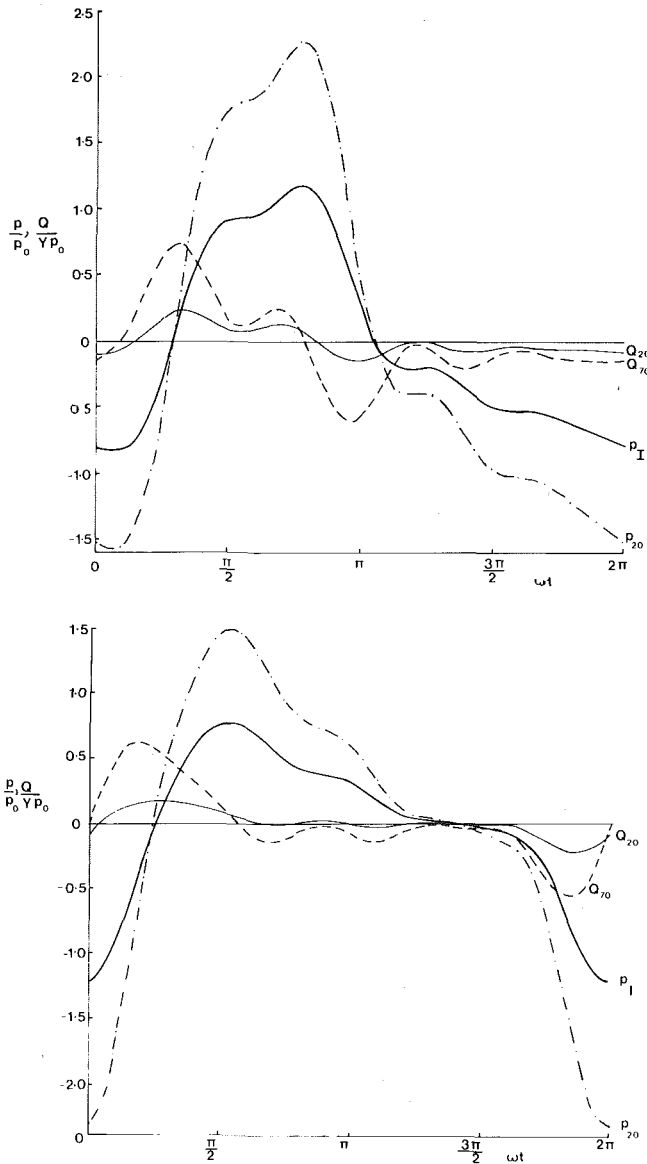


Fig. 2 Wave forms of dimensionless incident pressure (P_I , bold curve), total pressure at $l = 20$ mm (P_{20} , dash-dot curve), flow rate at $l = 20$ mm (Q_{20} , fine curve), flow rate at $l = 70$ mm (Q_{70} , broken curve), for $\alpha_1 = 0.05$ and $Q_o = Q_N$. (a) Waveform case 2, (b) waveform case 3.

al.'s experiments [16]. (The stenoses in Newman, et al.'s experiments were 3-4 mm long, and the distances upstream were given as approximate measurements, but any slight inaccuracy is unimportant for the qualitative comparisons presented here.) The input pressure wave form, $p_I(t)$, also has to be specified. Here we consider three cases: Case 1, a pure cosine wave; Cases 2 and 3 are pressure wave forms taken from McDonald's book [21, p. 163 and p. 154, respectively] and scaled so that the peak-to-trough amplitude is equal to 2; the latter are shown in Figs. 2(a, b), respectively. (Note that these waveforms include some contribution from peripheral reflections, so that their use as incident waveforms is quantitatively slightly unrealistic, although they are no less useful as examples.) For the purposes of calculation, it is convenient to specify these wave forms by the moduli and phases of their Fourier coefficients, P_{In} and ϕ_{PIn} in equation (11); in case 2 these were determined numerically from measured points on the wave forms, while in case 3 they were calculated from the quoted values for pressure gradient; in each case the values for the first five harmonics are given in Table 1, and the moduli are plotted in Fig. 3. (It is interesting

Table 1 Moduli and phases (in radians) of Fourier components of dimensionless incident pressure wave form

n	Case 2		Case 3	
	P_{In}	ϕ_{PIn}	P_{In}	ϕ_{PIn}
1	0.878	2.31	0.636	-2.91
2	0.353	-2.30	0.409	-1.48
3	0.020	-1.85	0.191	-0.53
4	0.134	-1.76	0.046	-0.01
5	0.077	0.55	0.046	0.51

to note that many authors give details of such moduli for their measured wave forms, but it is virtually impossible to find records of the phases.) Also, as the standard case, we take the mean flow rate Q_o to be equal to Q_N , making a comparison with the case where Q_o is given by equation (10).

As well as the incident wave form, Figs. 2(a, b) show the dimensionless pressure and flow-rate wave forms at $l = 20$ mm, and the flow-rate wave form at $l = 70$ mm, for the case $\alpha_1 = 0.05$. These are qualitatively similar to the experimental results of Newman, et al. [16] with the same value of α_1 , showing an amplification of the pressure wave just proximal to the stenosis and a very much reduced flow-rate wave form there compared with that at greater distances from the stenosis. This is entirely due to the presence of the reflected wave, as recognized by Newman, et al. [16], and also confirmed in their model calculations by Rooz, et al. [18]. We should note, however, that the enhanced amplitude of the proximal pressure wave was not reproduced in the femoral artery by Farrar, et al. [17], although the reduced flow-rate wave form certainly was.

The moduli of the Fourier harmonics of the reflected wave, p_{Rn} , are given for cases 1, 2, 3 and $\alpha_1 = 0.1$ in Fig. 3. The fact that there are contributions for $n \neq 1$ in case 1, the pure cosine wave, is a consequence of the nonlinearity of the stenosis head loss, which redistributes energy between different Fourier modes. In cases 2 and 3 this redistribution is somewhat obscured by the fact that there seems to be a rough proportionality between p_{Rn} and p_{In} in each case. That the proportionality is only very rough is exposed by Fig. 4, where the ratio between the reflected and incident moduli is plotted against n for the two cases 2 and 3 (and with $n = 1$ for case 1). The ratio of moduli for pressure and flow rate immediately distal to the stenosis is obtained by subtracting the plotted value from 1, and that for pressure immediately proximal by adding it to 1. The figure reveals two very important facts: (a) the modulus ratio depends markedly on frequency, which would not occur for a linear system (the linear results are also plotted on Fig. 4), and (b) its distribution with frequency is significantly different for the two wave forms used. Fact (a) appears to contradict the observations of Newman, et al. [15], although the scatter in their Fig. 4 was quite considerable; Farrar, et al. [17] did remark on this frequency dependence. Fact (b) does not seem to have been recognized explicitly before, although it is an obvious consequence of nonlinearity. It could by itself explain the discrepancies between the results for the aorta [15, 16] and those for the femoral artery [17], especially if the reflected wave is significantly re-reflected at the aortic trifurcation in the latter case.

This dependence on wave form is also manifest in plots against frequency of the modulus and phase of the input impedance of the system at a point proximal to the stenosis. Such plots are given in Fig. 5 for the case $\alpha_1 = 0.1$ and $l = 20$ mm. There is a slight fall with frequency of the modulus according to linear theory (closed circles) because 20 mm is not a negligible fraction of the wavelength (0.04) at the highest frequency involved (10 Hz, $n = 5$). There is also a monotonic phase variation. This is in marked contrast to the considerable frequency dependence according to nonlinear theory, and the great difference between the three wave forms

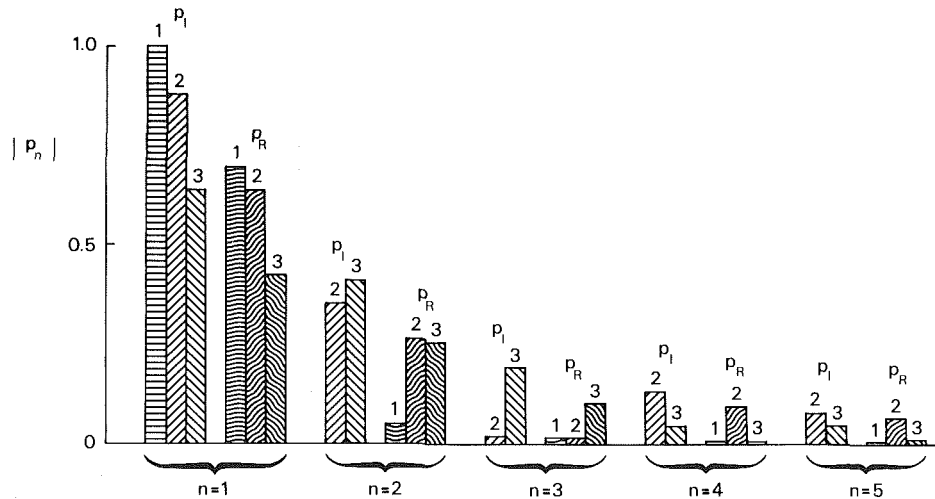


Fig. 3 Moduli of the first five Fourier coefficients of the dimensionless incident (p_i) and reflected (p_r) waves for $\alpha_1 = 0.1$ and $Q_o = Q_N$. Numbers 1, 2, 3 on the individual columns represent the three different incident waveforms (1 is the pure cosine wave, so there is no contribution to the incident waveform for $n > 1$).

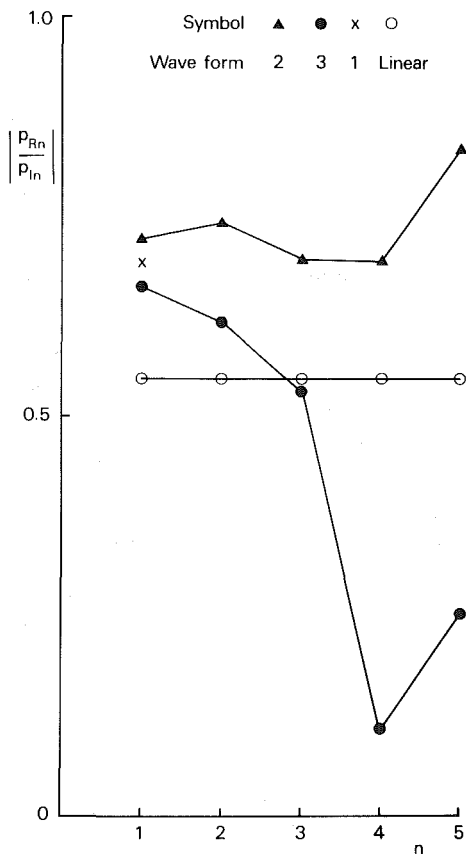


Fig. 4 Ratio of reflected to incident pressure wave modulus, plotted against harmonic number, n , for $\alpha_1 = 0.1$. All cases have $Q_o = Q_N$; results of a linear model are shown for comparison.

used. Also shown in Fig. 5 is the plot corresponding to case 2 when peripheral resistance is held constant, so Q_o is given by equation (10), instead of $Q_o = Q_N$. The difference is not large, and we may conclude that control of peripheral resistance does not have an important influence on the oscillatory parts of the wave form.

The effect on such impedance plots of varying α_1 and l is shown in Fig. 6, where only case 3 and only the case of constant peripheral resistance is considered. For all but the

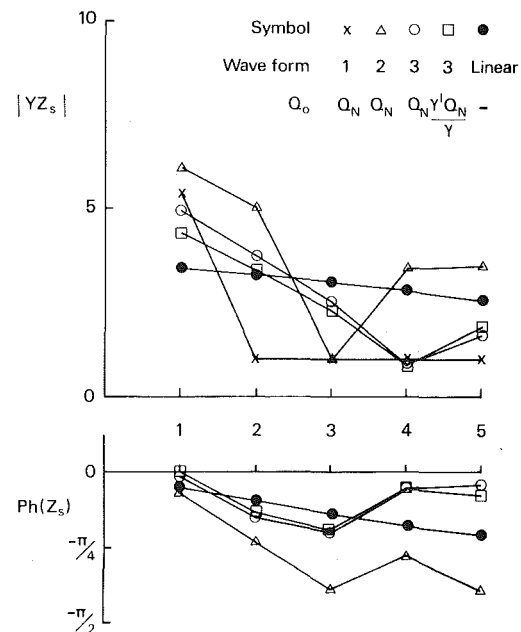


Fig. 5 Modulus and phase of dimensionless input impedance, plotted against harmonic number n , for $\alpha_1 = 0.1$, $l = 20$ mm, showing the effect of changing the incident waveform and the mean flow rate, compared with linear theory

severest stenoses ($\alpha_1 = 0.02$) the impedance modulus at $l = 20$ mm has a minimum at $n = 4$, while as the stenosis becomes more severe the impedance modulus of course increases for any n . Both these effects were observed by Farrar, et al. [17], and the latter by Newman, et al. [15]. Also, as the distance from the stenosis is increased (for $\alpha_1 = 0.1$), the impedance modulus falls, and the minimum is abolished; the shape of the curve at $l = 20$ mm agrees quite well with that for one of the dogs of Newman, et al. [16 fig. 5b], but the agreement deteriorates at larger values of l , no doubt because of the neglect in this model both of wave attenuation and of reflections from other parts of the arterial tree.

The phase of the impedance also shows a considerable variation with frequency, wave-form, α_1 and l (Figs. 5, 6). In most of the examples considered, the presence of the stenosis

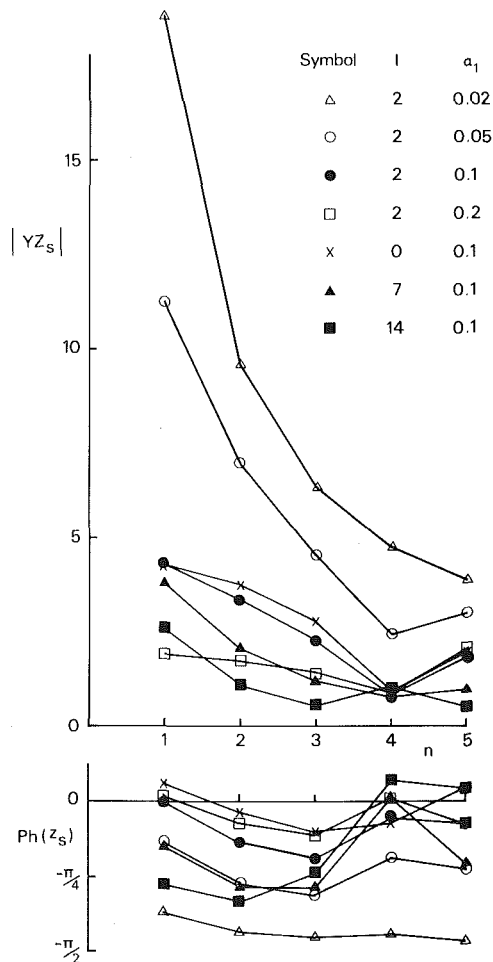


Fig. 6 Modulus and phase of dimensionless input impedance, plotted against harmonic number n , for wave form 3, $Q_0 = \gamma' Q_N / \gamma$, showing the effect of varying α_1 or l

causes the phase to become negative (flow-rate leading pressure) as is to be expected for a closed-end type of reflection. For the severest stenosis ($\alpha_1 = 0.02$) the phase angle is close to $-\pi/2$ at all frequencies considered (Fig. 6), as for a completely closed end. Figure 5 shows that in case 3 at $\alpha_1 = 0.1$ and $l = 20$ mm the phase is close to that predicted by linear theory when $n = 1, 2, 3$, but increases again for $n = 4, 5$.

Finally we follow Farrar, et al. [17, Fig. 4] and plot in Fig. 7(a) the peak-to-trough flow-rate amplitude at the stenosis ($l = 0$), divided by its value (2.0) in the absence of stenosis, and (b) the ratio of distal to proximal mean pressures (γ' / γ) (equivalent to the ratio of stenosed to normal mean flow rate in the case of constant peripheral resistance), against the severity of the stenosis ($1 - \alpha_1$). The results look very similar to those of Farrar, et al. [17] and confirm that although there has to be at least an 85 percent stenosis ($\alpha_1 < 0.15$) for the mean flow to be reduced by 10 percent, the amplitude is reduced by that amount for stenoses of 60 percent or more ($\alpha_1 < 0.4$).

Conclusion

The theory presented in this paper is physically comparable with, but mathematically and computationally simpler than, that of Rooz, et al. [18]. Like that model, it reproduces qualitatively many of the features observed experimentally by Newman, et al. [15, 16] and by Farrar, et al. [17] on the effect of stenoses of different severities on the pulse wave incident

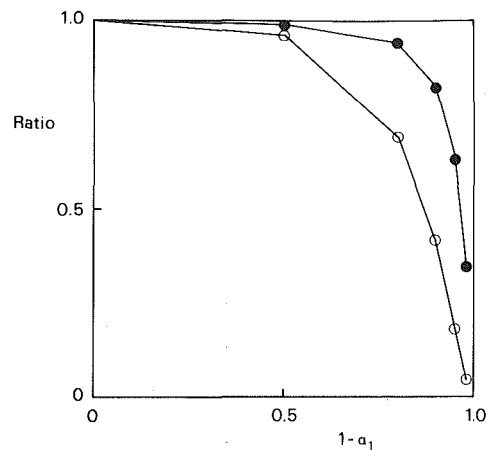


Fig. 7 Ratio of stenosed-to-normal mean flow rate (\bullet) and peak-to-trough flow-rate amplitude (\circ) plotted against severity of the stenosis ($1 - \alpha_1$), for waveform 3, $Q_0 = \gamma' Q_N / \gamma$, $l = 0$ mm

upon them. The main conclusion is that the frequency dependence of input impedance of such a nonlinear system may, for realistic physiological values of the various parameters, depend significantly on the shape of the incident wave form, as well as on the severity of the stenosis and the distance from it at which measurements are made. An experiment to investigate this in detail would be desirable. In order to apply such a model in vivo, however, it is important to know what can be regarded as given input. We have assumed that it is the incident pressure wave form and proximal mean pressure, but in fact we should match our model of the arterial tree, stenosis and all, to a model of the heart which incorporates the fact that it is neither a flow source nor a pressure source. The peripheral resistance (or, more properly, the input impedance of the peripheral circulation) also has to be known; but the evidence of Fig. 5 suggests that this may not make much difference to the effect of the stenosis on the proximal wave forms.

It would be simple in principle to extend this model in a number of ways, although to do so would make the computation more cumbersome and remove some of its advantage over the model of Rooz, et al. [18]. For example, the proximal and distal values of c and Y could be made different from each other without difficulty; in addition they could be made complex, to account both for wave attenuation in the artery, and for a compliance and inductance in the peripheral circulation. To do this realistically, however, these wave speeds and admittances would have to be made frequency dependent, so that Fourier analysis would have to be performed on the incident, reflected and transmitted waves even before the effect of the stenosis was considered, and the wave forms would have to be resynthesized before equation (9) could be used. Once such Fourier analysis had taken place, there would be no difficulty in including nonquasi-steady pressure drop across the stenosis ($K_n \neq 0$ in equation (6)), and in incorporating an artery with a stenosis as a branch in a network model, or in matching to a realistic heart model.

Finally we should note that the presence of a sphygmomanometer cuff will have an effect on the pulse wave in the brachial artery similar to that investigated here, and could therefore be one of the factors causing the recorded systolic and diastolic pressures to differ from the actual pressures [27]. Extension of the present theory to examine this effect can be made by allowing the severity of the stenosis, α_1 , itself to vary with time according to the instantaneous transmural pressure, although care must be taken not to neglect other collapsible tube effects that are important [28, Chapter 6].

Acknowledgment

I am very grateful to Dr. P. Sipkema for his constructive comments on the manuscript of this paper. A brief preliminary version was presented at the 3rd International Conference on Mechanics in Medicine and Biology, Compiègne, France in July 1982.

References

- 1 Clark, C., "The Propagation of Turbulence Produced by a Stenosis," *Journal of Biomechanics*, Vol. 13, 1980, pp. 591-604.
- 2 Deshpande, M. D., and Giddens, D. P., "Turbulence Measurements in a Constricted Tube," *Journal of Fluid Mechanics*, Vol. 97, 1979, pp. 65-89.
- 3 Khalifa, A. M. A. and Giddens, D. P., "Characterization and Evolution of Post-Stenotic Flow Disturbances," *Journal of Biomechanics*, Vol. 14, 1981, pp. 279-296.
- 4 Yongchareon, W., and Young, D. F., "Initiation of Turbulence in Models of Arterial Stenoses," *Journal of Biomechanics*, Vol. 12, 1979, pp. 185-196.
- 5 Duncan, G. W., Gruber, J. O., Dewey, C. F., Meyers, G. S., and Lees, R. S., "Evaluation of Carotid Stenosis by Phono-Angiography," *New England Journal of Medicine*, Vol. 293, 1975, pp. 1024-1028.
- 6 Strandness, D. E., Ward, K. J., Phillips, D. J., and Harley, J. D., "Evaluation of Carotid Disease by Various Noninvasive Methods," *Stroke*, Vol. 9, 1978, pp. 106-111.
- 7 Roach, M. R., "Poststenotic Dilatation in Arteries," *Cardiovascular Fluid Dynamics*, ed., D. H. Bergel, Vol. 2, Academic Press, London, 1972, pp. 111-139.
- 8 Fry, D. L., "Responses of the Arterial Wall to Certain Physical Factors," in *Atherogenesis: Initiating Factors*, eds., R. Porter and J. Knight, CIBA Foundation Symposium No. 12, Associated Scientific Publishers, Amsterdam, 1973, pp. 93-120.
- 9 Berguer, R., and Hwang, N. H. C., "Critical Arterial Stenosis: A Theoretical and Experimental Solution," *Annals of Surgery*, Vol. 180, 1974, pp. 39-50.
- 10 Young, D. F., and Tsai, F. Y., "Flow Characteristics in Models of Arterial Stenoses—I. Steady Flow," *Journal of Biomechanics*, Vol. 6, 1973, pp. 395-410.
- 11 Young, D. F., and Tsai, F. Y., "Flow Characteristics in Models of Arterial Stenoses—II. Unsteady Flow," *Journal of Biomechanics*, Vol. 6, 1973, pp. 547-559.
- 12 Young, D. F., Cholvin, N. R., and Roth, A. C., "Pressure Drop Across Artificially Induced Stenoses in the Femoral Arteries of Dogs," *Circulation Research*, Vol. 36, 1975, pp. 735-743.
- 13 Brice, J. G., Dowsett, D. J., and Lowe, R. D., "Haemodynamic Effects of Carotid Artery Stenosis," *British Medical Journal*, Vol. 2, 1964, pp. 1363-1366.
- 14 Young, D. F., Cholvin, N. R., Kirkeside, R. L., and Roth, A. C., "Haemodynamics of Arterial Stenoses at Elevated Flow-Rates," *Circulation Research*, Vol. 41, 1977, pp. 99-107.
- 15 Newman, D. L., Walesby, R. K., and Bowden, N. L. R., "Haemodynamic Effects of Acute Experimental Aortic Coarctation in the Dog," *Circulation Research*, Vol. 36, 1975, pp. 165-172.
- 16 Newman, D. L., Batten, J. R., and Bowden, N. L. R., "Partial Standing Wave Formation Above an Abdominal Aortic Stenosis," *Cardiovascular Research*, Vol. 11, 1977, pp. 160-166.
- 17 Farrar, D. J., Green, H. D., and Peterson, D. W., "Noninvasively and Invasively Measured Pulsatile Haemodynamics With Graded Arterial Stenosis," *Cardiovascular Research*, Vol. 13, 1979, pp. 45-57.
- 18 Rooz, E., Young, D. F., and Rogge, T. R., "A Finite-Element Simulation of Pulsatile Flow in Flexible Obstructed Tubes," *ASME JOURNAL OF BIOMECHANICAL ENGINEERING*, Vol. 104, 1982, pp. 119-124.
- 19 Womersley, J. R., "Oscillatory Flow in Arteries: The Reflection of the Pulse Wave at Junctions and Rigid Inserts in the Arterial System," *Phys. in Med. Biol.*, Vol. 2, 1958, pp. 313-323.
- 20 Newman, D. L., Westerhof, N., and Sipkema, P., "Modelling of Aortic Stenosis," *Journal of Biomechanics*, Vol. 12, 1979, pp. 229-235.
- 21 McDonald, D. A., *Blood Flow in Arteries*, 2nd Edition, Edward Arnold, London, 1974.
- 22 Caro, C. G., Pedley, T. J., Schroter, R. C., and Seed, W. A., *The Mechanics of the Circulation*, Oxford University Press, Oxford, 1978.
- 23 Kim, B. M., and Corcoran, W. H., "Analysis of Pressure Waves as a Means of Diagnosing Vascular Obstructions," *Med. and Biol. Engineering*, Vol. 11, 1973, pp. 422-429.
- 24 Lighthill, J., *Mathematical Biofluidynamics*, Chapter 12, Society for Industrial and Applied Mathematics, Philadelphia, 1975.
- 25 Elzinga, G., and Westerhof, N., "End-diastolic Volume and Source Impedance of the Heart," *The Physiological Basis of Starling's Law of the Heart*, eds., R. Porter and D. W. Fitzsimons, CIBA Foundation Symposium No. 24, Associated Scientific Publishers, Amsterdam, 1974, pp. 241-255.
- 26 Westerhof, N., Elzinga, G., Sipkema, P., and van den Bos, G. C., "Quantitative Analysis of the Arterial System and Heart by Means of Pressure-Flow Relations," *Cardiovascular Flow Dynamics and Measurements*, eds., N. H. C. Hwang and N. A. Normann, University Park Press, Baltimore, 1977, pp. 403-438.
- 27 Steinfeld, L., Alexander, H., and Cohen, M. L., "Updating Sphygmomanometry," *American Journal of Cardiology*, Vol. 33, 1974, pp. 107-110.
- 28 Pedley, T. J., *The Fluid Mechanics of Large Blood Vessels*, Cambridge University Press, Cambridge, 1980.